IEEE Access
Multidisciplinary | Rapid Review | Open Access Journal

Received 10 March 2024, accepted 19 March 2024, date of publication 27 March 2024, date of current version 3 April 2024.

Digital Object Identifier 10.1109/ACCESS.2024.3381219

RESEARCH ARTICLE

Direct Model Predictive Control of Fuel Cell and Ultra-Capacitor Based Hybrid Electric Vehicle

FARRUKH ZAIN UL ABIDEEN[1], HASSAN ABDULLAH KHALID[2], MUHAMMAD SAUD KHAN[1], HABIBUR REHMAN[3], (Member, IEEE), AND AMMAR HASAN[1,3]

[1]School of Electrical Engineering and Computer Science (SEECS), National University of Sciences & Technology (NUST), Islamabad 44000, Pakistan
[2]U.S.-Pakistan Center for Advanced Studies in Energy (USPCAS-E), National University of Sciences & Technology (NUST), Islamabad 44000, Pakistan
[3]Department of Electrical Engineering, American University of Sharjah, Sharjah, United Arab Emirates

Corresponding author: Ammar Hasan (amhasan@aus.edu)

This work was supported in part by the Open Access Program from the American University of Sharjah.

ABSTRACT Considering climate change, hybrid electric vehicles (HEVs) provide a clean alternative for transportation. This study presents an HEV with a fuel cell and ultra-capacitor connected in a parallel-type configuration. Direct model predictive control is used to optimize the power flow between the energy sources and the motor. Notably, the proposed controller uses a global approach, i.e., a single controller for the regulation of both power converters, thereby enhancing overall performance. Furthermore, the controller design leverages a non-averaged state space model that explicitly incorporates the switching nature of the converters. A method for computing reference currents for the fuel cell and ultra-capacitor is also introduced, which utilizes the ultra-capacitor current to manage power demand transients. Simulation results show that the proposed technique produces better results in terms of overshoot, steady-state error, and response time compared to recent studies in the literature.

INDEX TERMS Model predictive control (MPC), fuel cell (FC), ultra-capacitor (UC), hybrid electric vehicle (HEV).

I. INTRODUCTION

Conventional fossil fuel based vehicles have been around since the industrial revolution. However, the use of hydro-carbon fuel make these vehicles environmentally unfriendly & subsequently, worsen global warming on our planet [1], [2]. Hybrid electric vehicles (HEVs) & electric vehicles (EVs) present a ''green'' alternative to conventional vehicles. By adopting a personal carbon trading (PCT) system, the carbon footprint of the charging of EVs & HEVs from the grid, may be further minimized [3]. Moreover, cost of EV charging may be reduced by following a dynamic charging and discharging schedule [4]. Generally, HEVs use two or more kinds of energy sources to power the drive train. Common HEV combinations include internal combustion engine (ICE) with one or more energy sources such as battery, fuel cell (FC) and ultra-capacitor (UC) [5]. Though, batteries are considered environment friendly yet they need to be frequently charged externally for an EV and often for the HEV [6]. Commercially available batteries also suffer from low power density i.e., the ability to provide power quickly during sudden load transients [7], [8]. FC is a true environment-friendly option but suffers from the problem of slow power processing [9]. To overcome this problem, this work opts the combination of FC and UC for an HEV. None of these sources produce carbon emissions and hence are environmentally friendly [10]. FC is the main power source & UC is the auxiliary power source. A parallel-type topology has been selected, as shown in Fig. 1. The parallel topology ensures that both sources are able to provide energy simultaneously, when required. Other HEV topologies & configurations have been investigated in [11]. However, [11] does not focus on a control system, required to drive the HEV efficiently. A passive, cascaded configuration, including battery & UC as power sources, has been presented in [12]. Although the proposed topology is relatively straight-forward & does not use a control system, there is no control over the power usage of either source & hence, active power sharing between the sources is not possible. Similarly, a battery (main source) + UC (auxiliary source) configuration has been

The associate editor coordinating the review of this manuscript and approving it for publication was Guillermo Valencia-Palomo.

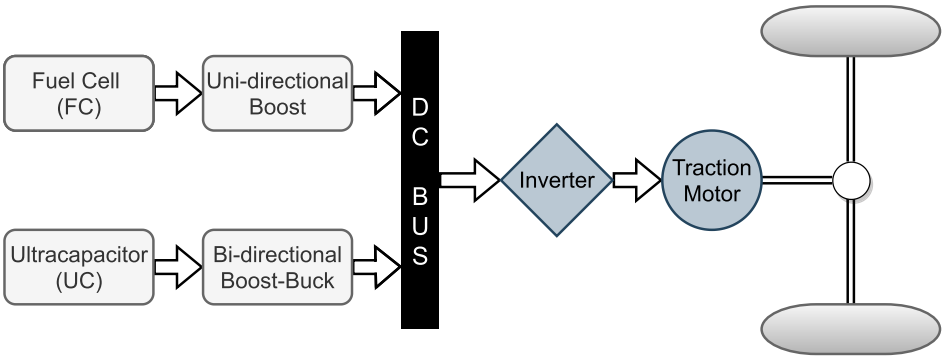

FIGURE 1. Layout of the selected FC-UC HEV.

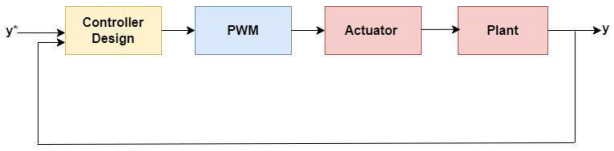

(a) Control Structure for PWM.

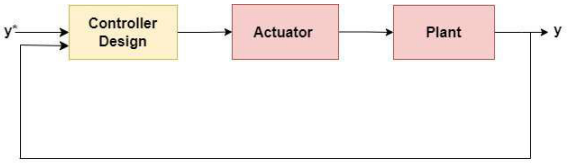

(b) Control Structure for Direct Finite Set.

FIGURE 2. Comparison of PWM and MPC control loops.

used in [13] and [14], in which the two energy sources are independently controlled, thus providing high flexibility. The selected parallel-type HEV topology has been considered in [15], [16], [17], and [18]. This topology uses two bidirectional DC-DC power converters, each for a battery (main source) & a UC (auxiliary source); hence, utilizing the recharging feature of both sources. It is superior configuration as it allows active power sharing, recharging through regenerative braking & voltage regulation of the DC bus [16].

Various control schemes, such as Lyapunov redesign [19], Backstepping control [16] and Integral Backstepping control [20] have also been proposed to control the selected system. Lyapunov redesign technique, which has high steady state error and slow response, uses the continuous state-averaged model. This model is basically an approximation and the control law needs to be re-derived whenever there is a variation in the mathematical model. Fuzzy logic based controller is proposed for FC/UC HEV, as in [21] and [22] which is simple but not robust. Additionally, the results are not compared with any standard driving cycles. Another study [23], proposes a complete ensemble empirical mode decomposition (CEEMD) fuzzy logic controller that confirms the state-of-charge (SOC) of UC and ensures that UC provides power in case of load variations. Although, CEEMD fuzzy logic control is accurate and robust, it is a complex control technique.

Model predictive control (MPC) controller consists of the broaden class of pre-calculating and prediction controllers. It is a subclass of predictive control which is widely used in electric drive systems and power electronic circuits [24], [25]. It belongs to numerous class of algorithms which uses the system model to calculate the best value of actuating variables. It calculates the system behavior for the case of sequence values, sets up to predict horizon and gives the best possible sequence at the minimal cost function [26], [27]. The cost function mainly consists of the control deviation. Generally, when the length of the prediction horizon (N) is large, it results in better control and robustness but at the cost of greater computational effort [28], [29], [30]. The proportional integral derivative (PID) controller usually calculates the reference values for the actuator which is based on the amplification of the control error. Classically, its tuning is done without the system knowledge [31]; however, intelligent tuning methods have also been introduced in the recent years [32]. Hence, MPC has various advantages over conventional control methods. Some are listed below:

- Ability to control multidimensional systems.
- Better handling of system constraints.
- Ability to control linear as well nonlinear systems

In electric drive systems and power electronics circuits, the time constants are in range of microseconds which require high sampling rate and greater processing power. In accordance with Moore's Law [33], the number of transistors on-chip increases doubles after every two years; hence, MPC can be easily implemented in the modern processors. There are many types of MPC that use the continuous value of control set. Some common types are generalized predictive control (GPC) which requires system identification methods, and finite-set MPC (FS-MPC) that uses a discrete mathematical model of the system [34]. The block diagram of Fig. 2(a) shows the pulse width modulation (PWM) control loop which requires a modulator. In contrast, there is no need for a modulator in FS-MPC as shown in Fig. 2(b). It evaluates and provides optimal switching sequence directly to the actuator. The cost function is formulated at each possible sequence and the least value

leads to the optimal sequence. This method can be extended to higher values of prediction horizon. Hence, if the system needs to be optimized in two steps then $2 \times 2 = 4$ switching combinations are evaluated, following the relation:

$$U = m^N$$

where, U is the optimal sequence and m is the number of switching states. So computational requirement for FS-MPC increases at higher values of N. However, MPC benefits from the predictive model to provide an optimal control input. It also offers a self-trending prediction in hydrogen electric multiple units (EMUs) [35]. Particularly, the proton exchange membrane fuel cell (PEMFC) is a complex non-linear system whose characteristics change as the connected load current changes. Since the conventional PID controller does not perform well under varying load conditions, MPC has been used instead in [36]. Results indicate better tracking operation using the MPC. The paper is arranged as follows: Section II presents the mathematical model of the FC-UC HEV & discusses its operation. Section III highlights the algorithm, used to implement the direct MPC. The simulation setup is provided in Section IV. Section V presents the simulation results and detailed discussion. Finally, the summary and concluding remarks are shared in Section VI of this paper.

II. DESCRIPTION OF THE MODEL

The selected HEV uses two energy sources, in parallel: (1) Fuel Cell & (2) Ultra-capacitor. FC produces DC voltage, when supplied with hydrogen fuel & cannot be recharged by conventional means. Moreover, the output voltage of FC is too low as compared to the voltage of the DC bus (V_{dc}). Therefore, a uni-directional DC/DC converter is required to step-up the FC voltage & to ensure that the power flows in only one direction. A boost converter does this job, as depicted in Fig. 1. In contrast, the UC can be discharged & recharged easily. Power from regenerative braking can be used to recharge the UC. Hence, a bi-directional DC/DC converter, called boost-buck, has been used with the UC, as shown in Fig. 1. The operation of the parallel FC-UC HEV is summarized below:

- FC is the main source, as it provides power to the DC bus continuously, as long as the vehicle is operating. Its output current is hence, considered positive.
- UC is the auxiliary source, as it is used to provide power during start-ups & times of high acceleration. In this state, its current is considered positive.
- UC can be recharged from regenerative braking, which is produced when the vehicle is either braking or slowing down. During this, its current is considered negative.
- Since the charge/discharge cycle of the auxiliary source repeats many times, a UC is preferred as it has 10 to 100 times more life cycles than a common battery [37]. Furthermore, the charge density of UC is higher than FC or battery i.e., it can discharge its energy way faster, which is useful in high acceleration of the vehicle.

Since the FC produces power as long as it is provided with the hydrogen fuel, it can be modeled as a DC voltage source. Similarly, in discharging mode, the UC can also be modeled as a DC voltage source. The models of UC & FC, along with the schematics of the DC/DC converters, are shown in Fig. 3.

Fig. 3 shows that the boost converter contains only one switch u_1, which is used to provide power from FC to DC bus. The boost-buck converter, on the other hand, enables bi-directional power flow, depending on the state of its switches u_2 & u_3, given as:

- Discharge (Boost) mode: $u_2 = 0, u_3 \in \{0, 1\}$
- Recharge (Buck) mode: $u_2 \in \{0, 1\}, u_3 = 0$

Using volt-second & charge-second balance, the continuous model of the FC-UC HEV has been derived in [16], given as:

$$\begin{aligned}
\dot{x}_1 &= \frac{V_{fc}}{L_1} - \frac{x_1 R_1}{L_1} - (1-u_1)\frac{x_3}{L_1} \\
\dot{x}_2 &= \frac{V_{uc}}{L_2} - \frac{x_2 R_2}{L_2} - (1-u_2)u_3\frac{x_3}{L_2} \\
\dot{x}_3 &= (1-u_1)\frac{x_1}{C_{dc}} + (1-u_2)u_3\frac{x_2}{C_{dc}} - \frac{I_o}{C_{dc}}
\end{aligned} \tag{1}$$

where, the variables correspond to the quantities shown in Fig. 3. In above, the state vector $\mathbf{x}$ is taken as:

$$\mathbf{x} = \begin{bmatrix} x_1 & x_2 & x_3 \end{bmatrix}^T = \begin{bmatrix} i_{fc} & i_{uc} & v_{dc} \end{bmatrix}^T \tag{2}$$

Depending on the values of the switches & the currents, the HEV operates in various modes. These modes are presented & described in Table 1.

Since direct MPC is a discrete control technique [38], the continuous model of eq. (1) is transformed into a discrete model using Euler approximation. The discrete model is given as eq. (3), shown at the bottom of the next page. The sampling time period has been represented by T_s in eq. (3). Eq. (3) is a non-averaged state-space model that is more accurate as it captures the switching dynamics of the converters.

III. DIRECT MODEL PREDICTIVE CONTROL (MPC)

The control scheme selected for this HEV model, is an enumeration-based MPC. It is comprised of three basic components: the discrete mathematical model of the plant, control objective and a receding horizon policy. The cost function (J) is evaluated using the discrete mathematical model of the system, given in eq. (3). Cost J is computed at every possible combination of the switches. The combination which produces the least valued J is selected as the best or the most optimal control input, at the current time instant k [39]. The receding horizon policy is the optimal strategy, planned over N time instants (k to $k + N$). However, only the present control input $u[k]$ is applied, whereas the rest is discarded. Afterwards, the horizon is shifted forward to the next N time instants [40]. Due to this, the MPC scheme is superior to other control schemes as it offers future prediction & dynamic disturbance rejection. The primary goal of MPC is to minimize the objective function. Hence, reference tracking

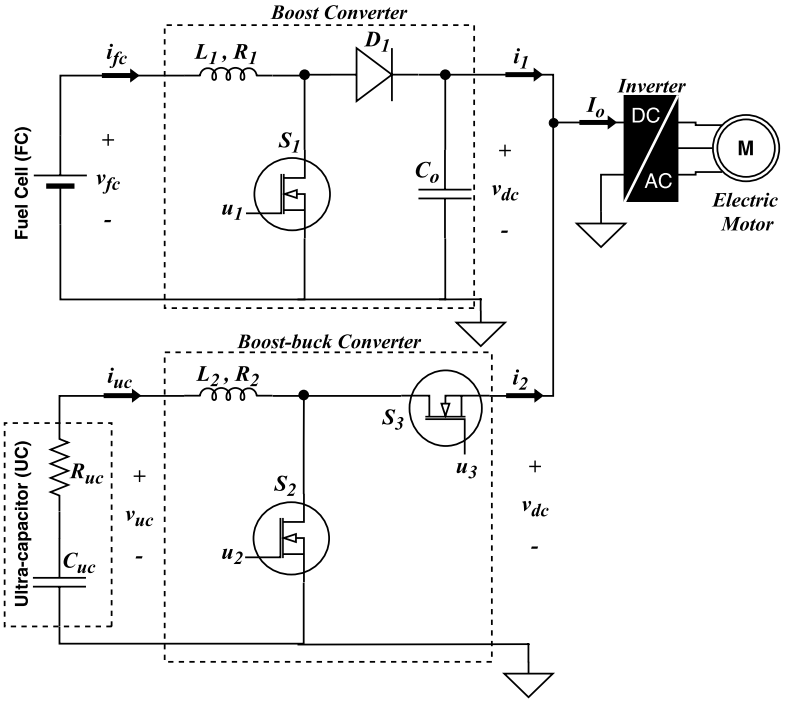

FIGURE 3. Schematic of the electrical side of the parallel FC-UC HEV.

TABLE 1. Modes of the FC-UC HEV.

No.	u_1	u_2	u_3	Currents	Description
1	0	0,1	0	$i_1 > 0, i_{uc} < 0, i_2 = 0$	FC provides power to DC bus; L_2 is negatively charging
2	0	0	1	$i_1 > 0, i_{uc} < 0, i_2 = i_{uc}$	FC provides power to DC bus; UC is charging
3	0	0	0,1	$i_1 > 0, i_{uc} > 0, i_2 = i_{uc}$	Both FC & UC provide power to DC bus
4	0	1	0	$i_1 > 0, i_{uc} > 0, i_2 = 0$	FC provides power to DC bus; L_2 is positively charging
5	1	0,1	0	$i_1 > 0, i_{uc} < 0, i_2 = 0$	C_{dc} provides power to DC bus; L_2 is negatively charging
6	1	0	1	$i_1 > 0, i_{uc} < 0, i_2 = i_{uc}$	C_{dc} provides power to DC bus; UC is charging
7	1	0	0,1	$i_1 > 0, i_{uc} > 0, i_2 = i_{uc}$	Both C_{dc} & UC provide power to DC bus
8	1	1	0	$i_1 > 0, i_{uc} > 0, i_2 = 0$	C_{dc} provides power to DC bus; L_2 is positively charging

can be achieved by introducing the error, between the desired state & its reference, in the objective function. Since, boost & boost-buck systems produce non-minimum phase behaviour on direct voltage control [19], an indirect current control is applied. Hence, the error variable introduced for FC current tracking is given in eq. (4):

$$e_{fc}[k] = i_{fc}^{ref}[k] - i_{fc}[k] \tag{4}$$

Similarly, the error variable introduced for UC current tracking is given in eq. (5):

$$e_{uc}[k] = i_{uc}^{ref}[k] - i_{uc}[k] \tag{5}$$

The average predictions of these errors are evaluated as eq. (6):

$$\begin{aligned} \bar{e}_{fc}[l|k] &= \frac{e_{fc}[l|k] + e_{fc}[l+1|k]}{2} \\ \bar{e}_{uc}[l|k] &= \frac{e_{uc}[l|k] + e_{uc}[l+1|k]}{2} \end{aligned} \tag{6}$$

where, l is the current prediction instant. The objective function J comprises of the error averages, shown in eq. (7):

$$J = \sum_{l=k}^{k+N-1} \frac{1}{N} \left|\bar{e}_{fc}[l|k] + \bar{e}_{uc}[l|k]\right| + \lambda|\Delta u[k]| \tag{7}$$

$$\begin{aligned} x_1[k+1] &= x_1[k] + T_s\left[\frac{V_{fc}}{L_1} - \frac{x_1[k]R_1}{L_1} - (1-u_1[k])\frac{x_3[k]}{L_1}\right] \\ x_2[k+1] &= x_2[k] + T_s\left[\frac{V_{uc}}{L_2} - \frac{x_2[k]R_2}{L_2} - (1-u_2[k])u_3[k]\frac{x_3[k]}{L_2}\right] \\ x_3[k+1] &= x_3[k] + T_s\left[(1-u_1[k])\frac{x_1[k]}{C_{dc}} + (1-u_2[k])u_3[k]\frac{x_2[k]}{C_{dc}} - \frac{I_o}{C_{dc}}\right] \end{aligned} \tag{3}$$

Eq. (7) shows that the objective function is evaluated over the entire horizon N. For each time instant, the average values of the errors are considered, using the current (l) & the next prediction ($l+1$) values. Furthermore, an error term of the control inputs $\Delta u[k]$ has been added along with a weighting factor $\lambda > 0$, to increase the stability of the system [38]. The term $\Delta u[k]$ is taken as the norm of the input error between the current & the previous time instants, as shown in eq. (8):

$$\Delta u[k] = \sqrt{\sum_{n=1}^{3} (u_n[k] - u_n[k-1])^2} \tag{8}$$

where, n represents the nth state & the maximum number of state variables in the system is three. The purpose of adding $\Delta u[k]$ is that it represents the past information about the selected inputs. The weighting factor λ can be increased or decreased to amplify or rectify the effect of the error input term. Manual tuning of λ may help to improve the accuracy of the results. Table 1 shows six distinct combinations of the control inputs $[u_1, u_2, u_3]$. Therefore, in each time instant, 6^N switching combinations are simulated, to predict the state variables over the entire horizon N i.e., the interval $[k+1, k+2, \ldots, k+N]$. J is evaluated for each switching combination & the optimal combination $\mathbf{u}^*[k]$ is selected for the minimum J, as given below:

$$\mathbf{u}^*[k] := \min(J)$$

The optimal input is then applied at the system to produce the results of the current time instant k. The process is repeated by shifting the fixed horizon over the next N time intervals. The pseudo-code of the proposed enumeration-based MPC is given below: The FC current reference i_{fc}^{ref} is calculated using the constant DC bus voltage reference V_{dc}^{ref} & the power balance equation, as given in eq. (9).

$$i_{fc}^{ref} = \beta \left(\frac{V_{dc}^{ref} I_o - V_{uc} i_{uc}^{ref}}{V_{fc}} \right) + p(V_{dc}) \tag{9}$$

where $p(V_{dc}) = K_p(V_{dc}^{ref} - V_{dc}) + K_i \int (V_{dc}^{ref} - V_{dc})$. The first term of eq. (9) is derived using the power balance equation in [19], where β is the ideality factor. The second term, $p(V_{dc})$ is proportional-integral term which is added to help reduce steady state error.

IV. SIMULATION

Using algorithm 1, a code is developed in MATLAB software that simulates the HEV model & implements the enumeration-based MPC on it. The operation of the code has been simplified using the flowchart of Fig. 4. The specifications of the HEV power sources, are configured in the simulation, as given in Table 2. Furthermore, the component values for the DC-DC converters, have been selected as depicted in Table 3. Various scenarios & types of references have been simulated using the MATLAB model. Results have been included in this document, along with detailed discussions on these results.

Algorithm 1 Direct Model Predictive Control (MPC) of FC-UC HEV

function MPC($\mathbf{x}$, U, i_{fc}^{ref}, i_{uc}^{ref}, N)
  Inputs:
    x = The state space values of dicrete-time model
    U = All possible switching combs. over N
    i_{fc}^{ref} = FC reference current
    i_{uc}^{ref} = UC reference current
    N = Fixed prediction Horizon
  Output:
    $\mathbf{u}^*$ = Optimal sequence of switching combs. over N

  for `all U over N` **do**
    $J = 0$
    for `l=k to k+N-1` **do**
      Compute $x(l+1)$ using eq. (3) & $u[k]$
      Compute $e_{fc}[k]$ & $e_{fc}[k+1]$ using eq. (4)
      Compute $e_{uc}[k]$ & $e_{uc}[k+1]$ using eq. (5)
      Compute $\bar{e}_{fc}[k]$ & $\bar{e}_{uc}[k]$ using eq. (6)
      Compute $\Delta u[k]$ using eq. (8)
      Compute J using eq. (7)
    end for
    $J_{array}(k) = J$
  end for
  $J_{optimal} = \min(J_{array})$
  $\mathbf{u}^* =$ **find** $(J_{optimal} in J_{array})$
end function

TABLE 2. Configuration of power sources.

Source	Specification
FC source	262 V, 200 A, 52 kW
UC source	205 V, 1500 F

TABLE 3. Parameter values.

Parameter	Values
Inductor L_1 and L_2	3.3 mH
Capacitance C_{dc}	1.66 mF
Resistance R_1 and R_2	20E-3 Ω

V. RESULTS AND DISCUSSION

This section presents the results of this study. Two different scenarios have been simulated in the MATLAB/Simulink software. The first one uses a test profile comprising of various reference levels, while the second scenario uses the standardized European urban driving cycle (EUDC) speed profile, provided as Fig. 5. The current reference profile is derived from the speed profile & shown in Fig. 6.

A. VARIABLE STEP REFERENCES FOR I_O & I_{UC}^{REF}

In this scenario, the performance of the designed HEV model is tested with variable output current demand I_o, as well as variable UC reference i_{uc}^{ref}, as shown in Table 4. Table 4 shows that the references have been set up to simulate various modes of acceleration, deceleration, UC charging & discharging, etc. This way, the model is tested to show the FC performance, charging/discharging capability of UC & active sharing of

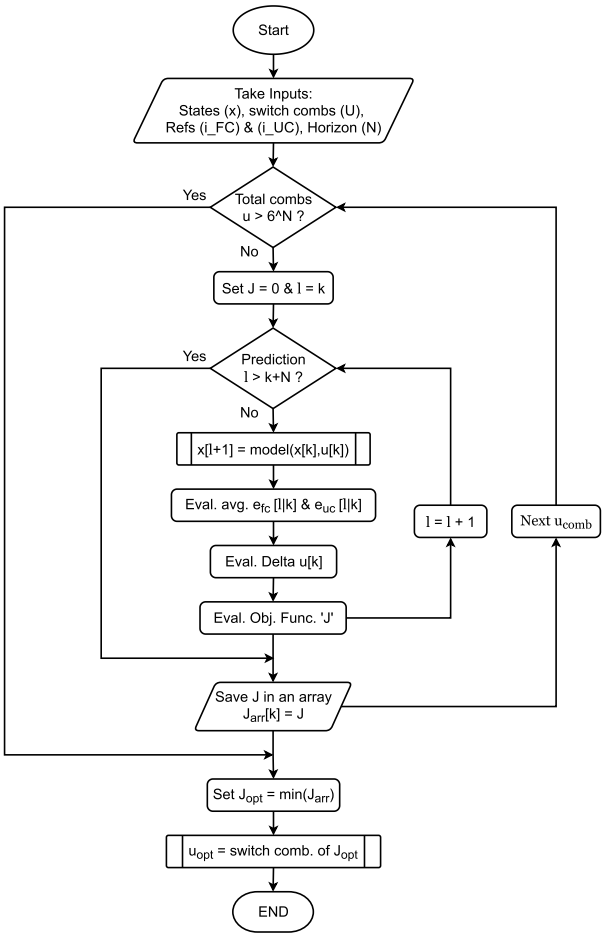

FIGURE 4. Flowchart of the MATLAB program, simulating the HEV model & the direct MPC.

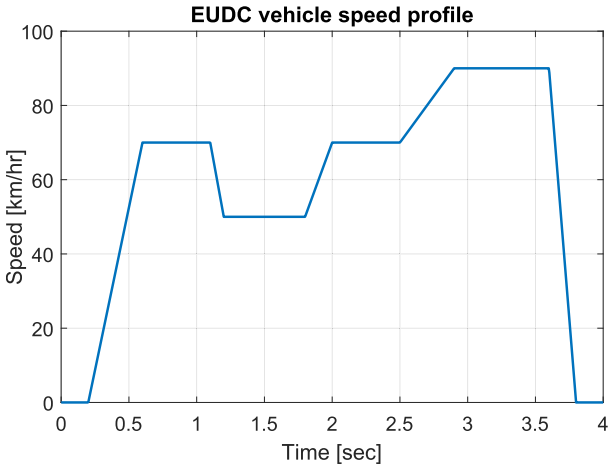

FIGURE 5. Speed profile of the vehicle, according to the EUDC standard.

power between FC & UC, to meet the required demand of I_o. Note that, the FC reference i_{fc}^{ref} has been generated at each time sample, using the relation evaluated in eq. (9). Relevant details about the simulation are listed in Table 5. After running the simulation, the graphs of i_{fc}, i_{uc} & V_{dc}

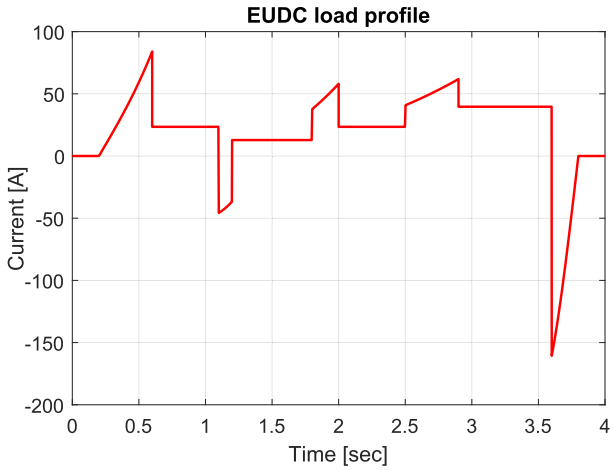

FIGURE 6. EUDC load current profile I_o.

TABLE 4. Simulated step references for scenario A.

Ref	$0 \leq t \leq 0.16$	$0.16 \leq t \leq 0.33$	$0.33 \leq t \leq 0.5$
I_o	50A (Normal)	70A (Acceleration)	30A (Deceleration)
i_{uc}^{ref}	10A (Start-up)	5A (Acceleration)	-3A (Regen. braking)
V_{dc}^{ref}	400V	400V	400V

TABLE 5. Simulation details.

Parameter	Value
Simulated time	0.5 sec
Time-step	1 μsec
Total execution time	8.1 sec
Number of horizon (N)	2

are obtained as Figs. 7, 8 & 9, respectively. The results indicate an initial overshoot at the start of the simulation, in all three states. The overshoot is comparatively large in Fig. 8. This is because the UC-buck boost converter starts in boost mode to provide power to the load. Large initial overshoot known as inrush current in boost converters is a well-known issue [41]. However, the overshoot dies down quickly as the states converge to their respective references, due to the controller action. The current waveforms of i_{fc} (Fig. 7) & i_{uc} (Fig. 8) show triangular signals of low amplitudes in steady-state, which is a characteristic of the non-averaged state space model. The waveform of i_{uc}^{ref} also shows negative current for simulation time $t \geq 0.33$ seconds, which indicates that the UC is being successfully charged by the regenerative braking. Fig. 9 shows a comparison of DC bus voltage V_{dc} from previous studies against the one obtained with the proposed technique. Comparison shows small overshoots at reference changes, quicker convergence, and lower steady-state error with the proposed method. A quantitative comparison between V_{dc} from the highlighted

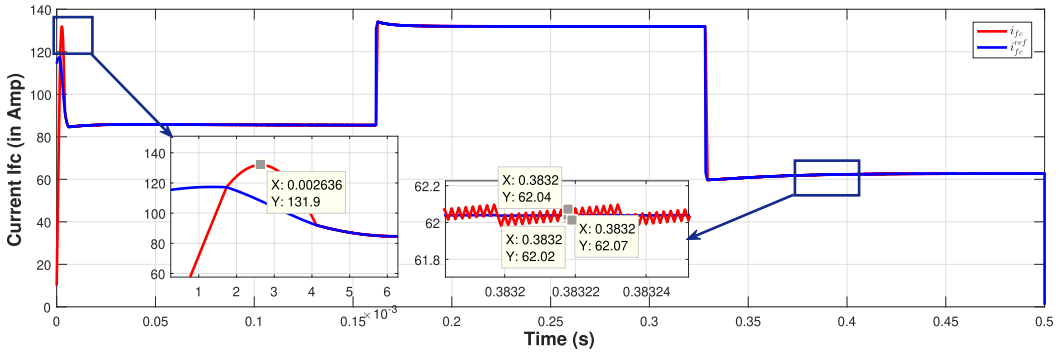

FIGURE 7. Graph of i_{fc} & its reference, for scenario A.

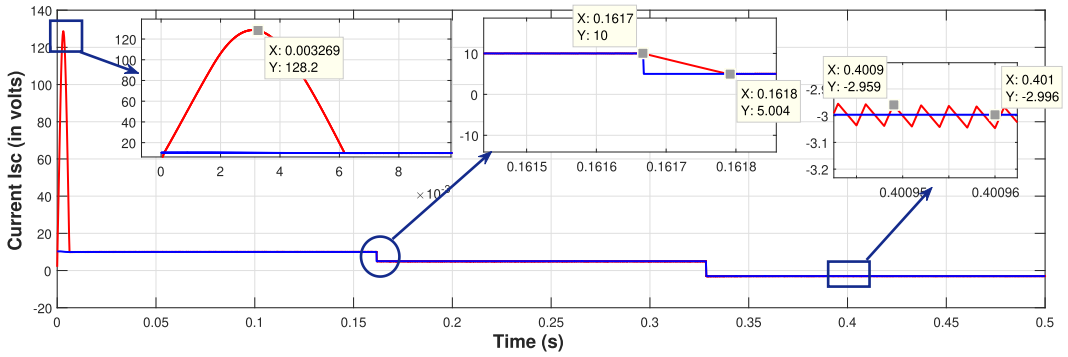

FIGURE 8. Graph of i_{uc} & its reference, for scenario A.

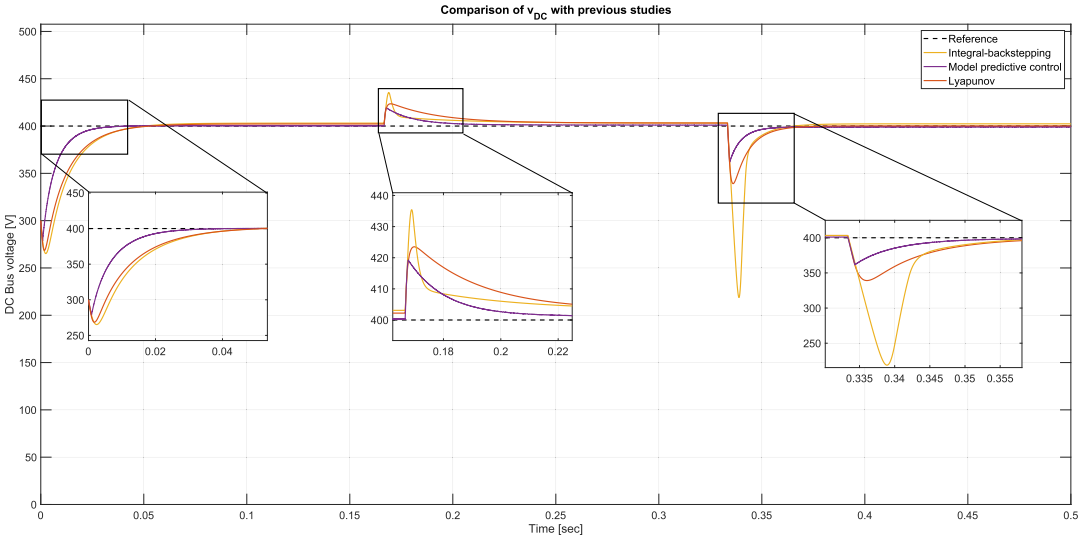

FIGURE 9. Comparison of V_{dc} with previous studies, for scenario A.

studies, is presented in Table 6. This comparison also shows better results for proposed method.

B. REFERENCE FROM EUDC

EUDC is a European standard driving cycle which emulates the performance of a vehicle, driving in an urban environment. Its speed profile is shown in Fig. 5. The speed profile (v_t) is translated to load current profile I_o using the relation:

$$I_o = \frac{v_t}{\eta V_{dc}^{ref}} \left[\frac{1}{2} \rho_{air} v_t^2 A C_x + M_t g C_r + M_t \frac{dv_t}{dt} \right] \quad (10)$$

The unknown parameters in eq. (10) are the physical specifications of the vehicle, assumed as the values given in Table 7. Using the values of Table 7, the load current

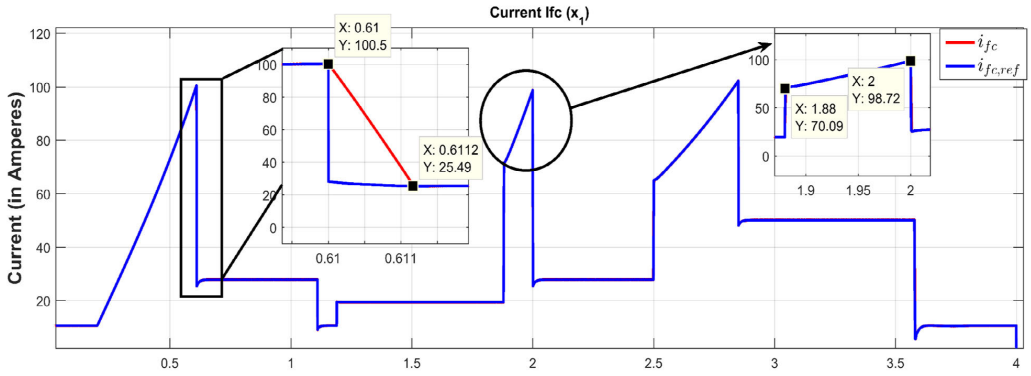

FIGURE 10. Graph of i_{fc} & its reference, for EUDC.

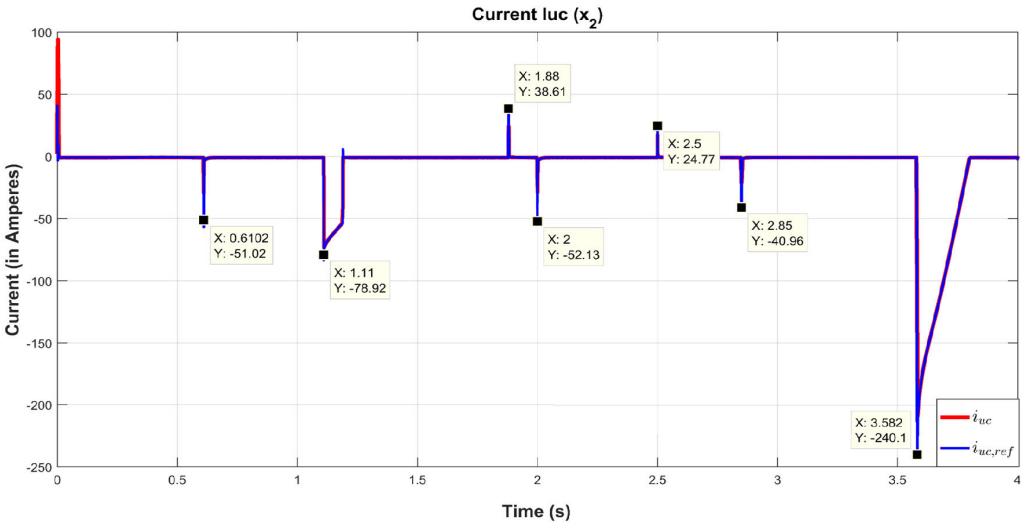

FIGURE 11. Graph of i_{uc} & its reference, for EUDC.

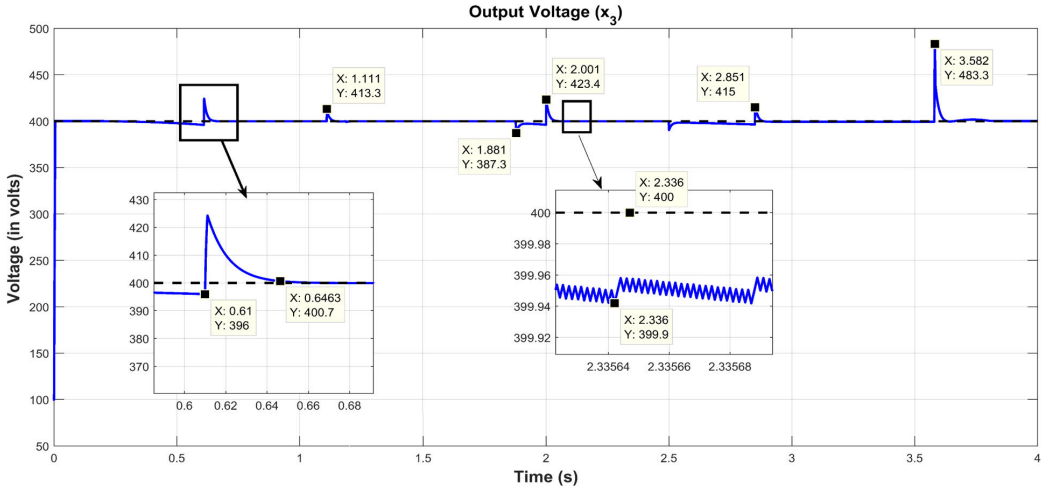

FIGURE 12. Graph of V_{dc} & its reference, for EUDC.

profile (I_o) is obtained as shown in Fig. 6. It can be seen in Fig. 6 that the time duration of the load profile I_o has been scaled down 100 times to reduce the time of the EUDC standard from 400 seconds to 4 seconds. This has been done

TABLE 6. Comparison of HEV output voltage V_{dc} against previous studies.

Technique	Initial overshoot	Response time	Steady state error
Lyapunov redesign [19]	421V	0.06 sec	4.5V
Integral backstepping [20]	0V	0.05 sec	3.2V
Model predictive control (MPC)	0V	0.03 sec	0.3V

TABLE 7. Specifications of the vehicle, its motor & inverter.

Specification	Symbol	Value
Mass of the vehicle	M_t	1922 kg
Aerodynamic drag coefficient	C_x	0.3
Front area of the vehicle	A	2.5 m^2
Rolling resistance coefficient	C_r	0.01
Acceleration due to gravity	g	9.8 m/s^2
Inverter efficiency	η	75%

to reduce the computational time of the simulation. Moreover, the reference currents of i_{fc}^{ref} & i_{uc}^{ref} have been proposed as eq. (11) & eq. (12), respectively.

$$\begin{aligned} i_{fc}^{ref} &= \frac{(I_o + I_{aux})V_{dc}^{ref}}{V_{fc}} + p(V_{dc}) \quad \text{For } I_o \geq 0 \\ i_{fc}^{ref} &= \frac{I_{aux}V_{dc}^{ref}}{V_{fc}} + p(V_{dc}) \quad \text{For } I_o < 0 \end{aligned} \tag{11}$$

$$i_{uc}^{ref} = \frac{(I_o + I_{aux})V_{dc} - i_{fc}V_{fc}}{V_{uc}} + \frac{1}{2}\frac{C_{dc}[(V_{dc}^{ref})^2 - (V_{dc})^2]}{0.01\ V_{uc}} \tag{12}$$

where, I_{aux} is the current of the auxiliary load of 2 kW, which has been introduced to give power to the vehicle in various modes. The first term of eq. (12) evaluates how much current is needed from the UC to provide/acquire power to the vehicle, whereas the second term is used to maintain the DC link voltage at constant V_{dc}^{ref}. Together, eqs. (11) & (12) utilize UC much effectively during the load demands of acceleration, deceleration, regenerative braking, etc. With DC bus reference of $V_{dc}^{ref} = 400$V, the waveforms of the states are shown in Figs. 10, 11 & 12.The waveforms of i_{fc} (Fig. 10) & i_{uc} (Fig. 11) show that the MPC controller successfully tracks the EUDC reference, with a very short settling time of a few microseconds. Plot of i_{uc} shows that it is positive (UC discharging) & negative (UC charging) at various times. Hence, the UC is charging & discharging, successfully. Plot of V_{dc} (Fig. 12) shows that transients are present at time instants when the change in the reference is very sharp. However, it settles down in a short time duration & a very small error of 0.05V persists in steady-state. Therefore, the successful reference tracking & an almost negligible steady-state error proves that the controller is performing precisely & accurately.

VI. CONCLUSION

In this study, a FC-UC HEV model is presented with an enumeration-based direct MPC. The HEV uses FC as its primary & UC as its auxiliary energy source. A non-averaged state space model of the HEV has been proposed, which exhibits characteristics (such as, current & voltage ripples) closer to an actual power converter. A global MPC is also proposed to match the global model of the HEV system. The performance of the proposed technique is tested in two different simulation scenarios: (1) step signals of variable amplitudes as current references, emulating various modes of the vehicle, such as, acceleration, deceleration, UC charging, UC discharging, etc., and (2) European extra-urban drive cycle standard, which is a standard testing reference, used in various studies to evaluate the performance of vehicle in urban setting. For the EUDC case, references for the states are generated using technique, proposed in (11) and (12), which utilizes UC much effectively during acceleration, deceleration & regenerative braking. In both scenarios, results show fast converging response & negligible steady-state errors. Comparison of the proposed technique with some of the previous studies, has been done visually in Fig. 9 & quantitatively in Table 6. The comparison indicates smaller overshoots, quicker response time & smaller steady-state error in the proposed scheme; hence, validating its superiority over the previous ones. It should be kept in mind that the performance of these control schemes heavily rely on their controller gains & may produce better results if the gains are fine-tuned. However, the designed MPC may produce better results because it is inherently more robust & better at disturbance rejection than some of these other control schemes.

ACKNOWLEDGMENT

This paper represents the opinions of the author(s) and does not mean to represent the position or opinions of the American University of Sharjah.

REFERENCES

[1] L. D. D. Harvey, *Global Warming*. Evanston, IL, USA: Routledge, 2018.
[2] K. Wang, J. Yang, C. Zhang, F. Wen, and G. Lu, "Joint energy-frequency regulation electricity market design for the transition towards a renewable-rich power system," *Int. J. Electr. Power Energy Syst.*, vol. 155, Jan. 2024, Art. no. 109504.
[3] L. Zhang, Q. Yin, W. Zhu, L. Lyu, L. Jiang, L. H. Koh, and G. Cai, "Research on the orderly charging and discharging mechanism of electric vehicles considering travel characteristics and carbon quota," *IEEE Trans. Transport. Electrific.*, early access, 2024, doi: 10.1109/TTE.2023.3296964.
[4] L. Zhang, C. Sun, G. Cai, and L. H. Koh, "Charging and discharging optimization strategy for electric vehicles considering elasticity demand response," *eTransportation*, vol. 18, Oct. 2023, Art. no. 100262.
[5] H. Marzougui, M. Amari, A. Kadri, F. Bacha, and J. Ghouili, "Energy management of fuel cell/battery/ultracapacitor in electrical hybrid vehicle," *Int. J. Hydrogen Energy*, vol. 42, no. 13, pp. 8857–8869, Mar. 2017.
[6] X. Li, Q. Wang, Y. Yang, and J. Kang, "Correlation between capacity loss and measurable parameters of lithium-ion batteries," *Int. J. Electr. Power Energy Syst.*, vol. 110, pp. 819–826, Sep. 2019.
[7] C. Choi, D. S. Ashby, D. M. Butts, R. H. DeBlock, Q. Wei, J. Lau, and B. Dunn, "Achieving high energy density and high power density with pseudocapacitive materials," *Nature Rev. Mater.*, vol. 5, no. 1, pp. 5–19, Oct. 2019.
[8] Y. Liang, C. Zhao, H. Yuan, Y. Chen, W. Zhang, J. Huang, D. Yu, Y. Liu, M. Titirici, Y. Chueh, H. Yu, and Q. Zhang, "A review of rechargeable batteries for portable electronic devices," *InfoMat*, vol. 1, no. 1, pp. 6–32, Mar. 2019.
[9] C. A. Ramos-Paja, A. Romero, R. Giral, J. Calvente, and L. Martinez-Salamero, "Mathematical analysis of hybrid topologies efficiency for PEM fuel cell power systems design," *Int. J. Electr. Power Energy Syst.*, vol. 32, no. 9, pp. 1049–1061, Nov. 2010.

[10] K. Rajashekara, "Hybrid fuel-cell strategies for clean power generation," *IEEE Trans. Ind. Appl.*, vol. 41, no. 3, pp. 682–689, May 2005.

[11] A. Emadi, Y. Joo Lee, and K. Rajashekara, "Power electronics and motor drives in electric, hybrid electric, and plug-in hybrid electric vehicles," *IEEE Trans. Ind. Electron.*, vol. 55, no. 6, pp. 2237–2245, Jun. 2008.

[12] J. Cao and A. Emadi, "A new battery/ultracapacitor hybrid energy storage system for electric, hybrid, and plug-in hybrid electric vehicles," *IEEE Trans. Power Electron.*, vol. 27, no. 1, pp. 122–132, Jan. 2012.

[13] X. Zhang, Y. Wang, X. Yuan, Y. Shen, Z. Lu, and Z. Wang, "Adaptive dynamic surface control with disturbance observers for battery/supercapacitor-based hybrid energy sources in electric vehicles," *IEEE Trans. Transport. Electrific.*, vol. 9, no. 4, pp. 5165–5181, 2022, doi: 10.1109/TTE.2022.3194034.

[14] X. Zhang, Z. Lu, X. Yuan, Y. Wang, and X. Shen, "L2-gain adaptive robust control for hybrid energy storage system in electric vehicles," *IEEE Trans. Power Electron.*, vol. 36, no. 6, pp. 7319–7332, Jun. 2021.

[15] A. Emadi, K. Rajashekara, S. S. Williamson, and S. M. Lukic, "Topological overview of hybrid electric and fuel cell vehicular power system architectures and configurations," *IEEE Trans. Veh. Technol.*, vol. 54, no. 3, pp. 763–770, May 2005.

[16] M. S. Khan, I. Ahmad, H. Armaghan, and N. Ali, "Backstepping sliding mode control of FC-UC based hybrid electric vehicle," *IEEE Access*, vol. 6, pp. 77202–77211, 2018.

[17] R. Faranda and S. Leva, "Energy comparison of MPPT techniques for PV systems," *WSEAS Trans. Power Syst.*, vol. 3, no. 6, pp. 446–455, 2008.

[18] D. Kumar and K. Chatterjee, "A review of conventional and advanced MPPT algorithms for wind energy systems," *Renew. Sustain. Energy Rev.*, vol. 55, pp. 957–970, Mar. 2016.

[19] H. El Fadil, F. Giri, J. M. Guerrero, and A. Tahri, "Modeling and nonlinear control of a fuel cell/supercapacitor hybrid energy storage system for electric vehicles," *IEEE Trans. Veh. Technol.*, vol. 63, no. 7, pp. 3011–3018, Sep. 2014.

[20] M. S. Khan, I. Ahmad, and F. Z. Ul Abideen, "Output voltage regulation of FC-UC based hybrid electric vehicle using integral backstepping control," *IEEE Access*, vol. 7, pp. 65693–65702, 2019.

[21] Y. Eren, O. Erdinc, H. Gorgun, M. Uzunoglu, and B. Vural, "A fuzzy logic based supervisory controller for an FC/UC hybrid vehicular power system," *Int. J. Hydrogen Energy*, vol. 34, no. 20, pp. 8681–8694, Oct. 2009.

[22] R. Dominguez, J. Solano, and A. Jacome, "Sizing of fuel cell—Ultracapacitors hybrid electric vehicles based on the energy management strategy," in *Proc. IEEE Vehicle Power Propuls. Conf. (VPPC)*, Aug. 2018, pp. 1–5.

[23] Y. Shen, J. Xie, T. He, L. Yao, and Y. Xiao, "CEEMD-fuzzy control energy management of hybrid energy storage systems in electric vehicles," *IEEE Trans. Energy Convers.*, vol. 39, no. 1, pp. 555–566, Mar. 2024.

[24] A. Linder, R. Kanchan, P. Stolze, and R. Kennel, *Model-based Predictive Control Electric Drives*. Göttingen, Germany: Cuvillier Verlag, 2010.

[25] L. Chen, D. Gao, and Q. Xue, "Energy management strategy for hybrid power ships based on nonlinear model predictive control," *Int. J. Electr. Power Energy Syst.*, vol. 153, Nov. 2023, Art. no. 109319.

[26] P. P. Karamanakos, "Model predictive control strategies for power electronics converters and AC drives," Ph.D. thesis, Tampere Univ., Tampere, Finland, Jul. 2013.

[27] A. M. Taher, H. M. Hasanien, S. H. E. A. Aleem, M. Tostado-Véliz, M. Ćalasan, R. A. Turky, and F. Jurado, "Optimal model predictive control of energy storage devices for frequency stability of modern power systems," *J. Energy Storage*, vol. 57, Jan. 2023, Art. no. 106310.

[28] P. Karamanakos, T. Geyer, and R. P. Aguilera, "Long-horizon direct model predictive control: Modified sphere decoding for transient operation," *IEEE Trans. Ind. Appl.*, vol. 54, no. 6, pp. 6060–6070, Nov. 2018.

[29] M. Abu-Ali, F. Berkel, M. Manderla, S. Reimann, R. Kennel, and M. Abdelrahem, "Deep learning-based long-horizon MPC: Robust, high performing, and computationally efficient control for PMSM drives," *IEEE Trans. Power Electron.*, vol. 37, no. 10, pp. 12486–12501, Oct. 2022.

[30] I. Prodan and E. Zio, "A model predictive control framework for reliable microgrid energy management," *Int. J. Electr. Power Energy Syst.*, vol. 61, pp. 399–409, Oct. 2014.

[31] P. Shah and S. Agashe, "Review of fractional PID controller," *Mechatronics*, vol. 38, pp. 29–41, Sep. 2016.

[32] R. P. Borase, D. K. Maghade, S. Y. Sondkar, and S. N. Pawar, "A review of PID control, tuning methods and applications," *Int. J. Dyn. Control*, vol. 9, no. 2, pp. 818–827, Jun. 2021.

[33] D. C. Brock, "Cramming more," in *Understanding Moore's Law: Four Decades of Innovation* (Integrated Circuits). Philadelphia, PA, USA: Chemical Heritage Foundation, 2006, p. 55.

[34] P. Karamanakos and T. Geyer, "Guidelines for the design of finite control set model predictive controllers," *IEEE Trans. Power Electron.*, vol. 35, no. 7, pp. 7434–7450, Jul. 2020.

[35] Q. Li, P. Liu, X. Meng, G. Zhang, Y. Ai, and W. Chen, "Model prediction control-based energy management combining self-trending prediction and subset-searching algorithm for hydrogen electric multiple unit train," *IEEE Trans. Transport. Electrific.*, vol. 8, no. 2, pp. 2249–2260, Jun. 2022.

[36] Q. Li, L. Yin, H. Yang, T. Wang, Y. Qiu, and W. Chen, "Multiobjective optimization and data-driven constraint adaptive predictive control for efficient and stable operation of PEMFC system," *IEEE Trans. Ind. Electron.*, vol. 68, no. 12, pp. 12418–12429, Dec. 2021.

[37] J. Bauman and M. Kazerani, "A comparative study of fuel-cell–battery, fuel-cell–ultracapacitor, and fuel-cell–battery–ultracapacitor vehicles," *IEEE Trans. Veh. Technol.*, vol. 57, no. 2, pp. 760–769, Mar. 2008.

[38] P. Karamanakos, T. Geyer, N. Oikonomou, F. D. Kieferndorf, and S. Manias, "Direct model predictive control: A review of strategies that achieve long prediction intervals for power electronics," *IEEE Ind. Electron. Mag.*, vol. 8, no. 1, pp. 32–43, Mar. 2014.

[39] P. Karamanakos, E. Liegmann, T. Geyer, and R. Kennel, "Model predictive control of power electronic systems: Methods, results, and challenges," *IEEE Open J. Ind. Appl.*, vol. 1, pp. 95–114, 2020.

[40] E. Carlos Garcia, D. M. Prett, and M. Morari, "Model predictive control: Theory and practice—A survey," *Automatica*, vol. 25, no. 3, pp. 335–348, May 1989.

[41] S.-C. Hsia, M.-H. Sheu, and J.-J. Jhou, "Fast-transient high-voltage buck-boost DC–DC conversion with low overshoot," *Microelectron. J.*, vol. 110, Apr. 2021, Art. no. 105016.

FARRUKH ZAIN UL ABIDEEN received the B.Sc. degree in electrical engineering specialization in power from the NFC Institute of Engineering and Technology, Multan, Pakistan, in 2016, and the master's degree in electrical engineering specialization in power and control systems from the School of Electrical Engineering and Computer Sciences (SEECS), National University of Sciences and Technology (NUST), Islamabad, Pakistan, in 2019, where he is currently pursuing the Ph.D. degree in electrical engineering with SEECS.

His research interests include non-linear control, optimal control techniques for control systems, model predictive control (MPC), hybrid electric vehicles (HEV), and maximum power point tracking (MPPT) of photovoltaic (PV) panels.

HASSAN ABDULLAH KHALID received the B.Sc. degree in electrical engineering from Air University, Islamabad, Pakistan, in 2007, the M.Sc. degree in electrical power engineering from the Chalmers University of Technology, Gothenburg, Sweden, in 2010, and the Ph.D. degree from the University of L'Aquila, L'Aquila, Italy, in 2016. He is currently an Associate Professor with the National University of Sciences and Technology. His current research interests include systems control with applications in power electronics, energy conversion, renewable energy, and smart grids.

MUHAMMAD SAUD KHAN received the master's degree in electrical engineering from the School of Electrical Engineering and Computer Science, National University of Science and Technology, Islamabad, Pakistan.

HABIBUR REHMAN (Member, IEEE) received the B.Sc. degree in electrical engineering from the University of Engineering and Technology at Lahore, Lahore, Pakistan, in 1990, and the M.S. and Ph.D. degrees in electrical engineering from The Ohio State University, Columbus, OH, USA, in 1995 and 2001, respectively.

He has a wide experience in the areas of power electronics, motor drives, and power systems in both industry and academia. From 1998 to 1999, he was a Design Engineer with the Ecostar Electric Drive Systems and Ford Research Laboratory, where he was a member of the Electric, Hybrid, and Fuel Cell Vehicle Development Programs. From 2001 to 2006, he was with the Department of Electrical Engineering, United Arab Emirates (UAE) University, Al Ain, United Arab Emirates, as an Assistant Professor. In 2006, he joined the Department of Electrical Engineering, American University of Sharjah, where he is currently a Professor. His primary research interests include power systems, power electronics, adjustable-speed drives, renewable energy systems, and alternative energy vehicles.

AMMAR HASAN received the B.E. degree in electrical engineering from the National University of Sciences and Technology, Islamabad, Pakistan, in 2004, and the master's and Ph.D. degrees in control systems from the Imperial College London, London, U.K., in 2008 and 2012, respectively. Since 2012, he has been with the School of Electrical Engineering and Computer Science, National University of Sciences and Technology. Currently, he is a Visiting Professor with American University of Sharjah. His research interests include model predictive control, control of power electronic converters, and optimization techniques for control systems.